

Huixing Zhang, Pedro D'Angelo Nunes, Michaela Wilhelm, Kurosch Rezwan

Hierarchically ordered micro/meso/macroporous polymer-derived ceramic monoliths fabricated by freeze-casting

Journal Article as: peer-reviewed accepted version (Postprint)

DOI of this document* (secondary publication): <https://doi.org/10.26092/elib/2496>

Publication date of this document: 29/09/2023

* for better findability or for reliable citation

Recommended Citation (primary publication/Version of Record) incl. DOI:

Huixing Zhang, Pedro D'Angelo Nunes, Michaela Wilhelm, Kurosch Rezwan,
Hierarchically ordered micro/meso/macroporous polymer-derived ceramic monoliths fabricated by
freeze-casting,
Journal of the European Ceramic Society, Volume 36, Issue 1, 2016, Pages 51-58, ISSN 0955-2219,
<https://doi.org/10.1016/j.jeurceramsoc.2015.09.018>

Please note that the version of this document may differ from the final published version (Version of Record/primary publication) in terms of copy-editing, pagination, publication date and DOI. Please cite the version that you actually used. Before citing, you are also advised to check the publisher's website for any subsequent corrections or retractions (see also <https://retractionwatch.com/>).

This document is made available under a Creative Commons licence.

The license information is available online: <https://creativecommons.org/licenses/by-nc-nd/4.0/>

Take down policy

If you believe that this document or any material on this site infringes copyright, please contact publizieren@suub.uni-bremen.de with full details and we will remove access to the material.

Hierarchically ordered micro/meso/macroporous polymer-derived ceramic monoliths fabricated by freeze-casting

Huixing Zhang, Pedro D'Angelo Nunes, Michaela Wilhelm*, Kurosch Rezwan

University of Bremen, Advanced Ceramics, Am Biologischen Garten 2, IW3, Germany

ARTICLE INFO

Article history:

Received 1 July 2015

Received in revised form

11 September 2015

Accepted 13 September 2015

Available online 26 September 2015

Keywords:

Hierarchical pore structure

Polysiloxanes

Freeze casting

Ice template

Silicon oxycarbide (SiOC)

ABSTRACT

A hierarchically-ordered macro/meso/microporous SiOC monolith was obtained via freeze-casting using commercial polysiloxane as a raw material and silica sol as a binder and template source. The pre-ceramic polymer polysiloxane was pyrolyzed at 600 °C to produce a hydrophilic surface; higher temperatures would fully decompose the organic groups. When silica sol and polysiloxane precursor were combined in freeze-casting method, after pyrolysis a polymer-derived SiOC ceramic monolith with a lamellar pore morphology and a hierarchically-ordered pore structure was obtained. Decomposition of the polysiloxane precursors results in the development of micropores, and particle packing is believed to be responsible for the mesopore formation. Macro/mesoporous hierarchically-ordered ceramics with a specific surface area of 74 m²/g are preserved at pyrolysis temperatures as high as 1000 °C. The influence of H44-derived filler amount (10 wt–40 wt%), freezing temperature (–20 °C, –80 °C, –150 °C), and pyrolysis temperature (600 °C, 700 °C, 1000 °C) on open porosity, pore size distribution, and surface characteristics were investigated.

1. Introduction

Macroporous monolithic ceramics may possess a high permeability with respect to gases and liquids and have found uses in a wide variety of industrial applications, including catalysis support [1], scaffolding for bone replacement [2], continuous flow capillary microreactors [3], filters for diesel soot [4], and liquid metal [5]. The incorporation of micropores (pore size <2 nm) and mesopores (2 nm < pore size < 50 nm) into a macroporous structure (pore size >50 nm) can combine improved mass transport with high surface area and large pore volumes, significantly broadening a material's range of applicability [6]. Fabrication of hierarchically-ordered porous ceramics normally involves the introduction of pores during preparation via some combination of the following methods: natural templating, surfactant templating, foaming, or freeze-casting [7–10].

Freeze-casting is a special kind of sacrificial templating method; the solvent solidifies and crystallizes (eg. ice) during the freezing process, sublimates, and leaves pores behind [11]. Freezing rate, solvents used, and precursor particle size will all have an influence on the final macroporous structure [12]. Water and organic

solvents, like camphene and *tert*-butyl alcohol, are commonly used for freeze-casting; the solvent used will influence the pore shape resulting from crystallization (eg. lamellar, cellular, or dendritic) [11,13,14]. Water is often used with inorganic ceramic powder suspensions (eg. Al₂O₃, SiC, SiO₂, ZrO₂) [11,15] and the green body obtained is then sintered to get a final macroporous monolith. For the preparation of SiC monolith using inorganic precursors, in order to get a mechanically strong monolith, sintering temperatures higher than 1400 °C are normally required [16,17]. For pre-ceramic precursors, camphene and *tert*-butyl alcohol have also been used to fabricate macroporous SiOC and SiC monoliths by freeze casting and pyrolysis [13,14].

The pre-ceramic precursors are polymers which can be converted into a ceramic material (SiC, SiCN, SiOC, etc.) by heat treatment in an inert atmosphere at temperatures in the range of 1000 to 1400 °C [18]. Polymer-derived ceramics, which are prepared at lower pyrolysis temperatures (500–1000 °C), have porosities at all pore diameter scales and surface characteristics [19,20]. Some studies on dendritic or cellular pore morphologies of SiOC or SiC ceramics by freeze-casting using preceramic polymer as precursor using camphene and *tert*-butyl alcohol has been performed [13,14]. However, the degree of cross-linking needs to be carefully monitored. Insufficient cross-linking will lead to poor mechanical integrity, and excessive cross-linking of polymer solution will cause gelation before freezing. To the best of our

* Corresponding author. Fax: +49 421 218 64932.

E-mail address: mwilhelm@uni-bremen.de (M. Wilhelm).

Table 1
Prepared materials and their composition, process, and pyrolysis parameters.

Material Denotation	H44 derived filler [wt%]	Silica sol ^a [wt%]	Freezing temperature [°C]	Pyrolysis temperature [°C] (-xxx)
H44-10 wt-150-xxx	10	90	-150	600/700/1000
H44-20 wt-150-xxx	20	80	-150	600/700/1000
H44-30 wt-150-xxx	30	70	-150	600/700/1000
H44-40 wt-150-xxx	40	60	-150	600/700/1000
H44-40 wt-80-xxx	40	60	-80	600/700/1000
H44-40 wt-20-xxx	40	60	-20	600/700/1000

^a Water content could be calculated based on the water content of silica sol (30 wt% silica, 70 wt% water). The solid phase includes H44-derived filler and silica nano-particles, and for samples with 10 wt%, 20 wt%, 30 wt%, and 40 wt% of H44-derived filler, solid loading equals to 37 wt%, 44 wt%, 51 wt%, 58 wt%, respectively.

knowledge, as of this writing, there are no studies combining pre-ceramic precursors with H₂O to prepare porous SiOC materials with a lamellar structure.

Hierarchical micro/macroporous SiOC monoliths have been fabricated by using a direct foaming method with polysiloxane in the authors' working group [21]. However, in this work, water is used as the pore templating agent, and polysiloxane is used as the precursor for the fabrication of lamellarly structured porous SiOC monoliths via freeze casting. A trimodal micro-/meso-/macroporous structure were created by combination of decomposition of pre-ceramic precursor with particle packing porosity and with ice templating. First, the surface characteristics of the polysiloxane precursor H44 was altered from hydrophobic to more hydrophilic by partially decomposed polysiloxane in an atmosphere of inert gas to "H44-derived filler" [22]. Then, this filler is mixed with silica sol, which is used as the binder and water-containing phase. The influences of the pyrolysis temperature, freezing temperature, and precursor composition on specific surface area, porosity, pore size distribution, and surface characteristics were studied. This method should enable the fabrication of large amounts of bulk monolith by reducing the very high volumetric shrinkage, and an appreciable density increase during polymer to ceramic conversion. Adapting the water-based freeze-casting method to the fabrication of polymer-derived ceramic monoliths offers the possibilities of generating a hierarchical pore structure with tailorable properties for different applications.

2. Experimental details

2.1. Material

A commercial methyl-phenyl polysiloxane powder (Silres® H44, Wacker Chemie AG) was used to prepare the H44-derived filler. Silica sol (SiO₂ nanoparticles, 8 nm, 30 wt% BegoSol® K, BEGO) was used as the binder and water-containing phase. Polyacrylic acid (PAA, Syntran 8140, Interpolymer) was added to adjust the pH value to ensure the complete condensation reaction of silica sol during the freezing process.

2.2. Processing

2.2.1. H44 derived fillers

The H44 was pre-cross-linked using a multi-stage heat treatment in air at 80 °C, 140 °C, and 200 °C (all dwell times 2 h), with a heating rate of 60 °C/h in between dwell times. The pre-cross-linked polysiloxane pieces were then pyrolyzed at 600 °C under a nitrogen atmosphere. The pyrolyzed samples were then ground with a grinder drive (MF 10 basic Microfine grinder drive, IKA) equipped with a 250 μm sieve grating. The resulting powder was then transferred to a planetary ball milling machine (PM 400, Retsch) and ground at 350 r/min for 4 h to produce a very fine powder.

2.2.2. Macroporous polymer-derived ceramic monolith

H44-derived fillers were added to silica sol in amounts as given in Table 1, and mixed with a rotating mixer. The pH of this suspension was adjusted to 6–7 by the addition of polyacrylic acid. The resulting slurry was then placed under vacuum to remove bubbles created during stirring, then quickly transferred to aluminium moulds and placed in freezers at various temperatures (given in Table 1) until completely frozen. In order to reduce thermal stress induced by heating, the frozen body was transferred to a -20 °C freezer for 1 hour and then to a -4 °C freezer for 3 h before drying in a climate chamber. The climate chamber was set to room temperature, with humidity between 85% and 95% for 5 days. During the drying step, more than 90% in the sample is removed, and residual water can be removed further during the cross-linking step. The "green bodies" were then cross-linked using a multi-stage heat treatment in air at 80, 140, and 200 °C (all dwell times 2 h), with a heating rate of 60 °C/h in between dwell times. Finally, the samples were pyrolyzed at various temperatures (given in Table 1) under an atmosphere of nitrogen. The preparation steps of the macroporous polymer-derived ceramic monoliths are shown in Fig. 1.

Sample compositions were varied during preparation by varying the weight ratio of H44-derived fillers (10–40 wt%) to silica sol (90–60 wt%). Three freezing temperatures and three pyrolysis temperatures were investigated: -150, -80, and -20 °C; and 600, 700, and 1000 °C, respectively. Full information, including sample nomenclature is given in Table 1. For example, the name H44-10 wt-150-xxx means that the weight percentage of H44-derived filler is 10%, the remaining 90% is silica sol, freezing temperature is -150 °C, and the sample was pyrolyzed at a temperature of xxx.

2.3. Characterization

Zeta potential was measured in order to get information on surface charges and to evaluate the stability of the suspension. Zeta potentials of the H44-derived filler were analysed using Dispersion Technology Zeta & Size 1200 (Dispersion Technology Inc). The morphology of the H44-derived filler and pyrolyzed samples was analysed via scanning electron microscopy (SEM, Camscan Series 2, Obducat CamScan Ltd.); sample specimens were first sputtered with gold (K550, Emitech, Judges Scientific plc.). Macroporosities of the monoliths were determined via mercury intrusion porosimetry (Pascal 140/440, POROTEC GmbH). Specific BET surface areas and BJH pore size distributions were determined by nitrogen adsorption and desorption isotherms measured at 77K using a Belsorp-Mini (Bel Japan, Inc.). The samples were degassed at 120 °C for 3 h. Before degassing, the monolith materials were ground and sieved with a 300 μm mesh sieve in order to minimize nitrogen diffusion effects during the measurements. Water vapour and *n*-heptane adsorption measurements were carried out by placing vessels with ~0.5 g of sample powder (particle sizes ≤300 μm) inside closed Erlenmeyer flasks filled with the solvent at equilibrium with its vapour phase at room temperature. Samples were weighed at the start and end of a 24 h measurement period in order to determine the vapour uptake

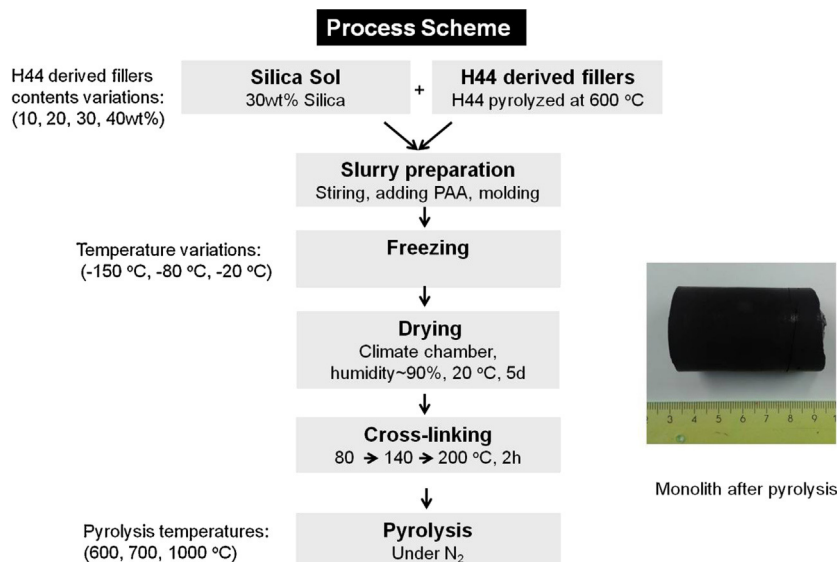


Fig. 1. Process scheme, parameter variation of synthesized samples and monolithic structure of pyrolyzed sample.

of the material. Later, the uptake was recalculated into g/m^2 using the BET surface of the materials.

3. Results

3.1. Properties of H44-derived fillers

The H44 precursor, which contains phenyl and methyl groups, is very hydrophobic. Thus, the properties of H44-derived fillers had to be modified in order to allow them to mix with water during freeze casting. When the H44 precursor is pyrolyzed at 600 °C, the decomposition of phenyl group occurs, resulting in a hybrid material. Pre-pyrolyzed H44, which could not cross-link further (only if are some -OH groups remaining), and act to fill the space, is therefore referred to as H44-derived filler.

The planetary ball milling machine was used to reduce the particle size of the H44-derived filler; in freeze-casting, the filler particle size greatly influences the pore structure [12]. Dynamic light scattering measurements indicated a particle size range from 100 to 1000 nm, however, they display a tendency to aggregate, as shown in Fig. 2a.

A surface charge on the particle was created predominantly by the decomposition of phenyl groups during pyrolysis at 600 °C. When the particles are mixed with water, the absolute value of the zeta potential can indicate the stability of the suspension. Values between 1 and 10 mV indicate unstable suspensions, values between 10 and 30 mV indicate that the suspension exhibits initial, temporary particle stability in de-ionized water [23,24], and values above 30 mV suggest that the suspension is very stable. For the H44-derived filler suspended in water, the absolute value of zeta potential is found to be more than 10 mV, shown in Fig. 2b, indicating a initial stability (up to 1 h; the freezing process takes only a few minutes at -150 °C).

Compared to water, the negatively charged H44-derived fillers had higher stability in anionic colloidal silica, due to stronger inter-particle repulsion. The pH value of the slurry also influences the zeta potential of particles, and thus the suspension stability. A slurry pH value of 6 to 7 was experimentally determined to produce the mechanically strongest monoliths after freezing. The cross-linking (condensation) rate between silica particles is greatly influenced by the pH of the slurry; this effect allows silica to act as a binder during the preparation process. A pH value below 6 led to suspensions having very low stability, while pH values of 8 to 11 lead to insufficient

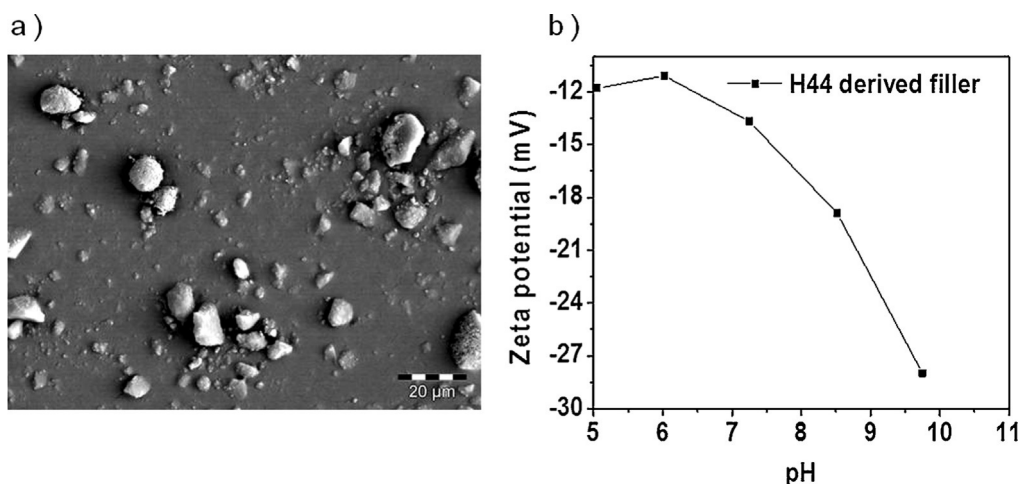


Fig. 2. (a) SEM images of H44-derived fillers after planetary milling at 350 r/min for 4 h. (b) Zeta potential of the H44-derived filler in de-ionized water.

a) H44-40wt-150-1000

b) H44-40wt-80-1000

c) H44-40wt-20-1000

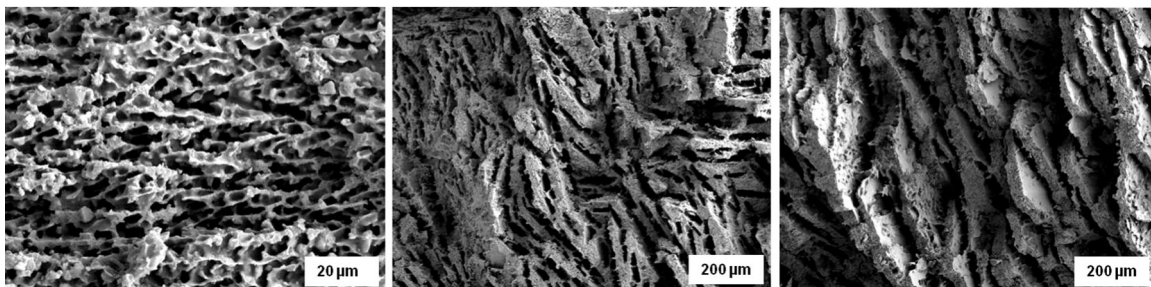


Fig. 3. SEM images of pyrolyzed monoliths with different freezing temperatures. Horizontal length of the white boxes represents the sizes given therein.

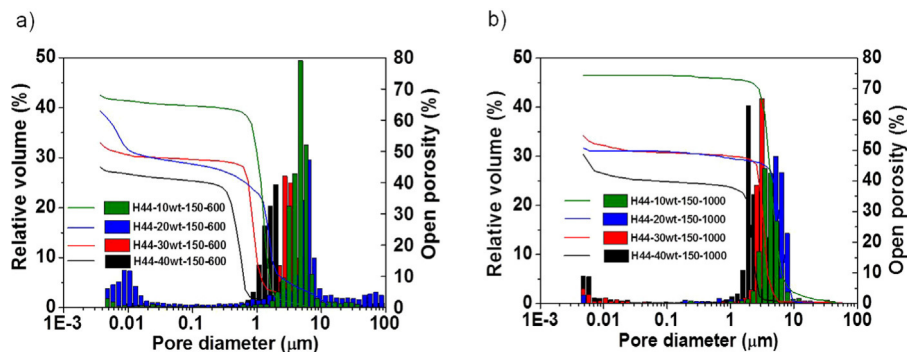


Fig. 4. Pore size distribution versus relative pore volume (coloured columns) and open porosity curves (coloured lines) obtained from Hg-porosimetry of pyrolyzed samples: (a) Samples with different H44-derived filler amounts, pyrolyzed at 600 °C; (b) Samples with different precursor ratios, pyrolyzed at 1000 °C.

cross-linking of silica sol during freezing process. When the slurry was prepared with a pH >11, gelation occurred before freezing could commence. Radial shrinkage of samples pyrolyzed at 600 °C, 700 °C, and 1000 °C, was observed to be 3%, 4%, and 11% respectively.

Powder XRD analysis (Supplement Fig. 1) confirms that the final product is structurally amorphous (no SiC or SiO₂ peaks are detected). SiOC is not a single stoichiometric phase, but instead built from nanodomains of amorphous SiO₂ and carbon; the material produced in this work is a SiOC material, having varying carbon contents and domain sizes. Wherein the sample contains especially for high contents of silica particles, it may also be described as SiO₂ nanoparticles embedded in a SiOC ceramic matrix.

3.2. Pore structure and porosity

3.2.1. Effect of freezing temperature on pore structure

The pore structure and porosity depends heavily on the freezing process. During freezing, the ice crystals tend to nucleate at the bottom surface of the cylindrical mould, growing upwards along the axis. However, due to the low thermal conductivity of the H44-derived filler materials, ice crystal growth inward from the circumference of the mould quickly comes to dominate the growth structure of the monolith. The ice growth forms anisotropic pore structures [25].

The pore structures of the monolith are shown in Fig. 3. The pore morphologies of pyrolyzed monoliths differ with changes in freezing temperature (varied freezing rates). The samples, which were frozen at -150 °C, display a tubular (also described in other literature as “columnar”) pore structure, while the samples frozen at -80 °C and -20 °C, show a lamellar pore structure. The pore sizes increase with increasing freezing temperature (decreased freezing rate). The pore diameters of H44-derived samples range from less than 10 μm (-150 °C), to 20 μm (-20 °C). Fig. 3c shows how the wall is constructed from particles, which are the H44-derived filler

materials. The macropore size can also be analyzed with Hg intrusion porosimetry, which provides additional information about the porosity.

Fig. 4 shows the results of the Hg-intrusion porosimetry of pyrolyzed samples having various amounts of H44-derived filler. The detected macropore sizes exhibit very narrow distributions, and all of the pore sizes fall into the range of 1 to 10 μm. This indicates that a very uniform pore size is produced by freeze casting, similar to other pore sizes found in literature [26]. The increase in H44-derived filler amounts (and simultaneous decrease in water content) leads to lower porosity and smaller pore size. When the filler amounts varied from 10 wt% (further decreases lead to poor monolith structure) to 40 wt% (further increases result in an inhomogeneous suspension), open porosity decreases from 70 to 45%. Additionally, pore diameters shift to a lower average value; around 5 to 1 μm. Similar trends occur with samples pyrolyzed at 700 and 1000 °C, as shown in Fig. 4b. Notably, the solid phase includes H44-derived filler and silica nanoparticles; samples having 10, 20, 30, and 40 wt% H44-derived filler content, together with silica nanoparticles constitute, respectively, 37, 44, 51, and 58 wt%. Since porosity is determined by the solid volume, it will decrease with increasing H44-derived filler. Fig. 4a and b demonstrate that the pyrolysis temperatures used had no obvious influence on the macroporous structure in terms of pore size and porosity.

3.3. Specific surface area and hierarchical structure

3.3.1. Effects of solid loading and pyrolysis temperature

The presence of hysteresis loops in the nitrogen adsorption and desorption isotherms in Fig. 5a indicates a mesoporous structure in all of the samples even after pyrolysis at 1000 °C. However, the microporous component of the structure is only stable up to 700 °C; pyrolysis at 1000 °C results in an almost complete collapse of the micropores. Macroporosity is normally preserved at higher

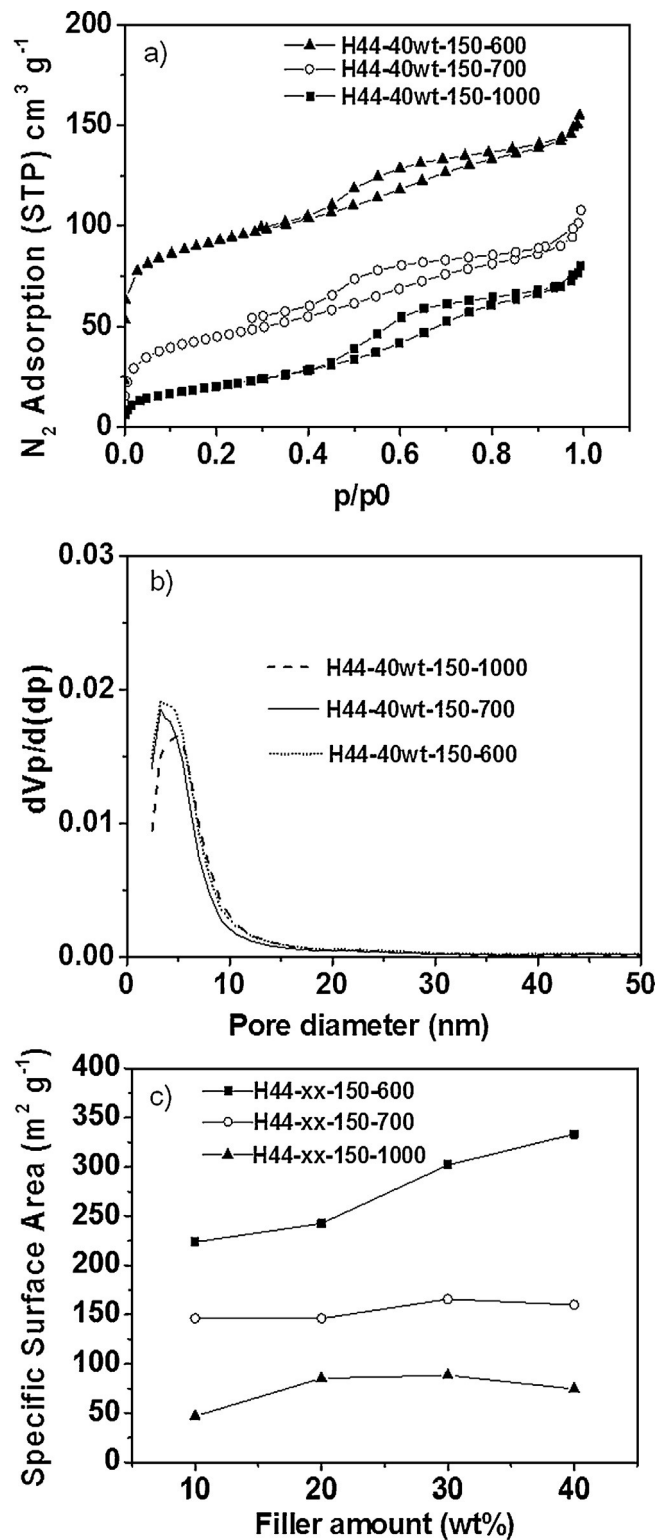


Fig. 5. (a) Nitrogen adsorption-desorption isotherms for samples with 40 wt% H44-derived filler, pyrolyzed at different temperatures. (b) BJH analysis of pore size distribution. (c) Specific BET surface areas of pyrolyzed (600/700/1000 °C) monoliths as determined by nitrogen adsorption for samples with varied H44-derived filler loadings.

pyrolysis temperatures [27]. BJH analysis (Fig. 5b) indicates mesopore diameters between 2 and 12 nm. Interestingly, mesopore size and count seem not to be influenced significantly by pyrolysis temperature, as can be observed by the shape of the hysteresis loop in Fig. 5a, and the BJH plots in Fig. 5b.

The influence of H44-derived filler amounts on specific surface area (SSA) was also studied (Fig. 4c). It can be seen that the SSA could

be influenced by changes in the amounts of added filler, and varied from 46.8 to 350 m^2/g . At a pyrolysis temperature of 600 °C, with the H44-derived filler amounts increasing from 10 to 40 wt%, the SSA increased from 220 to 350 m^2/g . Using a pyrolysis temperature of 700 °C, the SSA rose from 146.2 to 159.8 m^2/g with increasing H44-derived filler amounts. After a pyrolysis at 1000 °C, the SSA

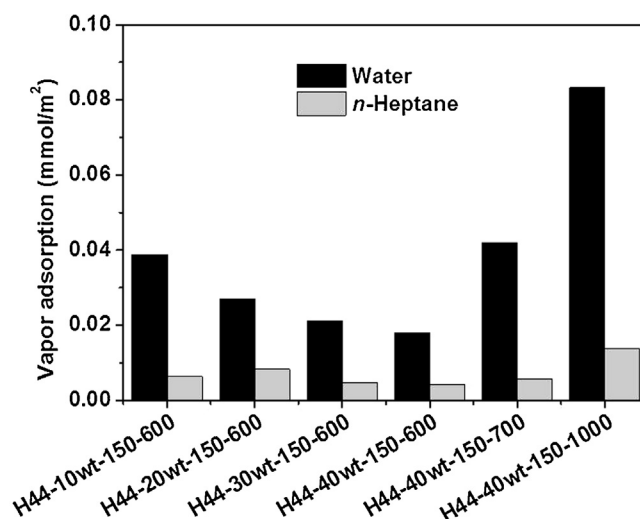


Fig. 6. Water and *n*-heptane vapor adsorption at 25 °C for samples with different H44-derived filler amounts pyrolyzed at 600 and 700 °C. The sorption data were recalculated using the specific BET surface area from N₂ adsorption.

still increased, rising from 46.8 to 74.4 m²/g with increasing filler amount.

3.4. Surface characteristics

Hydrophilicity and hydrophobicity characteristics of the pyrolyzed samples are indicated by water and *n*-heptane vapour adsorption at 22 °C (Fig. 6). All of the samples obtained display hydrophilic surface characteristics. Depending on the pyrolysis temperature and the H44-derived filler amounts, the hydrophilicity varies. Higher pyrolysis temperatures (1000 °C) lead to the decomposition of methyl groups in the precursor, resulting in improved surface hydrophilicity of the pyrolyzed sample. This is indicated by greater amounts of water vapour adsorbed per SSA, compared to the *n*-heptane adsorption. The water vapour adsorption greatly increased with increasing pyrolysis temperature, from 0.019 to 0.084 mmol/m², compared to *n*-heptane adsorption: 0.005 to 0.015 mmol/m². For samples pyrolyzed at 600 °C, when the filler amount increases from 10 wt% to 40 wt%, the more hydrophilic silica content decreases, resulting in an overall decrease in the water adsorption with increasing filler content.

4. Discussion

4.1. Lamellar morphology of SiOC materials

The surface characteristics of polymer precursors can be adjusted by preliminary pyrolysis. Initial work has shown that H44 precursor pyrolyzed at 500 °C still exhibits a very hydrophobic surface based on water and *n*-heptane adsorption results. After

pyrolysis at 600 °C, the resultant filler material's surface displays more hydrophilic characteristics (see Supplemental Fig. 2). This enables the formation of the suspension with water. Pyrolysis at higher temperatures would increase the hydrophilicity slightly, but lead to a higher degree of decomposition of the H44 precursor. This would reduce the carbon content in the final SiOC material and monolith mechanical strength.

Unlike polysiloxane dissolving in an organic solvent, such as camphene, in which the pore structure is created by a thermally-induced phase separation of solvent from solute [28], the pore structure is created by H44-derived filler material pushed aside by ice crystals as they grow. During the freezing process, the particles in the slurry are repelled by the moving ice solidification front, concentrated, and trapped in between the growing ice crystals. The now-agglomerated silica particles will undergo a cross-linking reaction and act as a binder, forming a mechanically strong monolith. It has been reported that at high solid contents, a tubular (or columnar) pore structure is produced during the freeze casting process [12,29]. The pore morphologies of pyrolyzed monoliths differ when frozen at different temperatures; structures varied from tubular pores to lamellar pores. Macropore structures did not change during pyrolysis.

Water crystallizes in the hexagonal crystal system, with the ice crystals having a growth velocity approximately 100 times faster in the *a*-direction of the hexagonal base than in the perpendicular *c*-direction [30]. As a result, ice crystals develop a lamellar microstructure parallel to the *a*-direction, resulting in a lamellar spacing. Lower freezing temperatures result in higher freezing front velocities. For the samples freezing at -150 °C, the higher freezing velocity lead to smaller ice lamellae. The ice growth along the *c*-axis

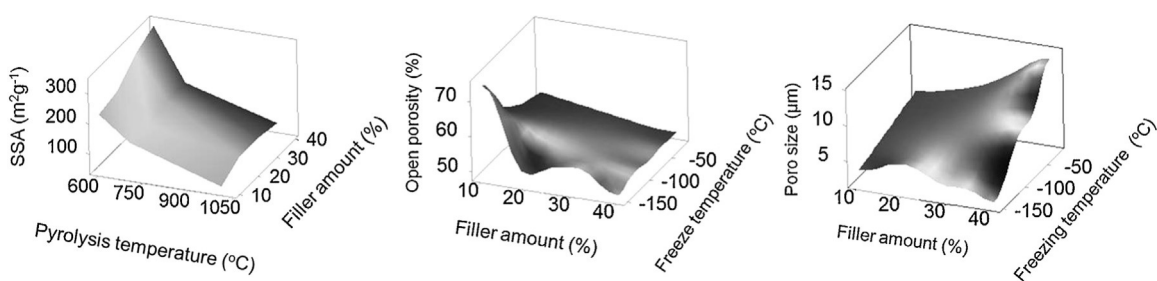


Fig. 7. (a) 3D representation of the influence of filler amount and pyrolysis temperatures on SSA. (b) Influence of filler amounts and freezing temperatures on porosity. (c) Influence of factors from 7b on pore size.

bridged lamellar pores and resulted in a tubular channel structure. Conversely, wall thickness increased greatly with warmer freezing temperatures, due to lower numbers of ice crystal nucleations and a lower ice front velocity at slower freezing rates [12].

4.2. Hierarchical structure

The freeze-casting method by itself can only produce macroporous structures. However, by combining freeze-casting with the pre-ceramic polymer, micropores were introduced via decomposition of the pre-ceramic polymer [22]. Additionally, the packing geometry of the H44-derived filler with silica particles and itself results in the formation of a mesoporous structure [31]; the sizes of the particles directly influence the pore size. The H44-derived filler particles fall into the sub-micron range, which normally should produce pores in the same size range. However, during the pyrolysis of the green body, the silica particles and H44 derived filler may still react [32]. This allows the particles to bind together, reducing the 'particle packing' pore size, and maximizing the mechanical strength of the final monolith. Thus, it is important that the preliminary pyrolysis temperature not exceed 600 °C to get mechanically strong monolith. As shown in Fig. 5, mesopores appeared to be unaffected by pyrolysis temperatures from 600 to 1000 °C, likely due to the relative stability of the H44-derived filler material at these temperatures (see TGA results in Supplemental Fig. 3). Additionally, silica particles are well embedded in the ceramic matrix, which suppresses silica particle growth (silica particles not embedded in a ceramic matrix are expected to coarsen greatly at the applied temperature of 1000 °C). This phenomenon is often observed for particles embedded in a carbon matrix [33]. The usage of silica sol also plays an important role in the mechanical strength of the monolith.

4.3. Influences of the process parameters

SSA measured by nitrogen adsorption and desorption, open porosity and pore size measured by Hg intrusion were plotted against pyrolysis temperature, H44-derived filler amount, and freezing temperature, respectively. The 3D visualization in Fig. 7 shows that the pyrolysis temperature has more influence on SSA than amounts of H44-derived filler. The highest SSA is obtained for materials with a filler amount of 40 wt% pyrolyzed at 600 °C. The freezing temperature was found to have very little impact on SSA (not shown). The reason for the adjustable SSA is the H44-derived filler, which exhibits a SSA of around 500 m²/g for the pristine material pyrolysed at 600 °C [22,34]. Due to the relatively high amount of H44-derived filler in the monolith, increasing the filler amount can, to a point, increase the SSA. At pyrolysis temperatures of 1000 °C, micropores are destroyed, and mesopores are still preserved, the less contribution of mesopores to SSA resulting in a reduction of SSA gains with increasing filler percentages.

The main factors influencing the resultant morphology and porosity are the freezing temperature and solid loading; also observed for materials derived from inorganic powders [12]. Increases in solid content of the suspension at the same freezing temperatures result in slightly smaller ice crystals, due to a lowered water content. Both H44-derived filler amount and freezing temperature influence the open porosity and pore size. For porosity, filler amount plays a major role. However, for the sample H44-10 wt-xx-1000, when frozen at -20 °C, a much larger pore size and thicker pore walls resulted. The extremely high water content led to a very fragile monolith structure, which collapsed easily into powder. The pore structure might be partially destroyed during the drying process, leading to the low porosity. In some studies that have used camphene and *tert*-butyl alcohol as the solvent, solid loading influenced pore size dramatically [13]. However, in

this study, pore size was not strongly influenced by filler amount, likely due to the rapid crystallization of water compared to other solvents. The highest porosity can be achieved with lowest filler amounts at lowest freezing temperature.

5. Conclusion

Polymer-derived ceramic monoliths with hierarchically-ordered micro-/meso-/macroporous structures have been fabricated for the first time using a water-based freeze-casting method and polysiloxane-based filler as the solid phase. The hierarchically-ordered pore structure, pore size distribution, porosity, SSA, surface characteristics can be adjusted by varying pyrolysis temperatures, solid loadings, and freezing temperatures. The combination of polymer-derived filler materials with freeze-casting not only results in lamellar SiOC structures (pore sizes from a few up to ca. 20 μm), but is also responsible for a relatively high SSA (46.8 m²/g to 350 m²/g) in the presence of mesopores (diameters of 2 to 12 nm). Using H44-derived filler material as the solid phase enables the fabrication of bulk monoliths, free of cracks. The hierarchically-ordered structure, in combination with adjustable material properties, like surface characteristics, could be enormously advantageous for applications such as gas separation and liquid filtration.

Acknowledgments

This work was supported by German Research Foundation (DFG) within the Research Training Group GRK 1860 "Micro-, meso- and macroporous nonmetallic Materials: Fundamentals and Applications" (MIMENIMA).

Appendix A. Supplementary data

Supplementary data associated with this article can be found, in the online version, at <http://dx.doi.org/10.1016/j.jeurceramsoc.2015.09.018>.

References

- [1] U.F. Vogt, L. Györfy, A. Herzog, T. Graule, G. Plesch, Macroporous silicon carbide foams for porous burner applications and catalyst supports, *J. Phys. Chem. Solids* 68 (2007) 1234–1238.
- [2] H. Seitz, W. Rieder, S. Irsen, B. Leukers, C. Tille, Three-dimensional printing of porous ceramic scaffolds for bone tissue engineering, *J. Biomed. Mater. Res. B Appl. Biomater.* 74B (2005) 782–788.
- [3] K.F. Bolton, A.J. Canty, J.A. Deverell, R.M. Guijt, E.F. Hilder, T. Rodemann, J.A. Smith, Macroporous monolith supports for continuous flow capillary microreactors, *Tetrahedron Letters*. 47 (2006) 9321–9324.
- [4] J. Adler, Ceramic diesel particulate filters, *Int. J. Appl. Ceram. Technol.* 2 (6) (2005) 429–439.
- [5] Z. Taslicukur, C. Balaban, N. Kuskonmaz, Production of ceramic foam filters for molten metal filtration using expanded polystyrene, *J. Eur. Ceram. Soc.* 27 (2007) 637–640.
- [6] P. Colombo, C. Vakifahmetoglu, Stefano costacurta, fabrication of ceramic components with hierarchical porosity, *J. Mater. Sci.* 45 (2010) 5425–5455.
- [7] Y. Shin, C. Wang, Gregory J. Exarhos, Synthesis of SiC ceramics by the carbothermal reduction of mineralized wood with silica, *Adv. Mater.* 17 (2005) 73–77.
- [8] Y.S. Shin, J. Liu, J.H. Chang, Z.M. Nie, Gregory J. Exarhos, Hierarchically ordered ceramics through surfactant-templated sol-gel mineralization of biological cellular structures, *Adv. Mater.* 13 (2001) 728–732.
- [9] X.J. Mao, S.W. Wang, S. Shimai, Porous ceramics with tri-modal pores prepared by foaming and starch consolidation, *Ceram. Int.* 34 (2008) 107–112.
- [10] A.Z. Lichtner, D. Jauffrès, D. Roussel, F. Charlot, C.L. Martin, R.K. Bordia Dispersion, connectivity and tortuosity of hierarchical porosity composite SOFC cathodes prepared by freeze-casting, *J. Eur. Ceram. Soc.* 35 (2015) 585–595.
- [11] A.R. Studart, U.T. Gonzenbach, E. Tervoort, L.J. Gauckler, Processing Routes to Macroporous Ceramics: A Review, *J. Am. Ceram. Soc.* 89 (6) (2006) 1771–1789.
- [12] S. Deville, Freeze-casting of porous ceramics: A review of current achievements and issues, *Adv. Eng. Mater.* 10 (2008) 155–169.

- [13] M. Naviroj, S.M. Miller, P. Colombo, K.T. Faber, Directionally aligned macroporous SiOC via freeze casting of preceramic polymers, *J. Eur. Ceram. Soc.* 35 (2015) 2225–2232.
- [14] B.H. Yoon, E.J. Lee, H.E. Kim, Highly aligned porous silicon carbide ceramics by freezing polycarbosilane/camphene solution, *J. Am. Ceram. Soc.* 90 (6) (2007) 1753–1759.
- [15] L.F. Hu, C.A. Wang, Y. Huang, C.C. Sun, S. Lu, Z.J. Hu, Control of pore channel size during freeze casting of porous YSZ ceramics with unidirectionally aligned channels using different freezing temperatures, *J. Eur. Ceram. Soc.* 30 (2010) 3389–3396.
- [16] M. Fukushima, M. Nakata, Y. Zhou, T. Ohji, Y. Yoshizawa, Fabrication and properties of ultra highly porous silicon carbide by the gelation–freezing method, *J. Eur. Ceram. Soc.* 30 (2010) 2889–2896.
- [17] B.H. Yoon, C.S. Park, H.E. Kim, In situ synthesis of porous silicon carbide (SiC) ceramics decorated with SiC nanowires, *J. Am. Ceram. Soc.* 90 (12) (2007) 3759–3766.
- [18] P. Colombo, M. Modesti, Silicon oxycarbide ceramic foams from a preceramic polymer, *J. Am. Ceram. Soc.* 82 (3) (1999) 573–578.
- [19] P. Colombo, G. Mera, R. Riedel, G.D. Soraru, Polymer-derived ceramics: 40 years of research and innovation in advanced ceramics, *J. Am. Ceram. Soc.* 93 (7) (2010) 1805–1837.
- [20] P. Colombo, Engineering porosity in polymer-derived ceramics, *J. Eur. Ceram. Soc.* 28 (2008) 1389–1395.
- [21] H. Schmidt, D. Koch, G. Grathwohl, P. Colombo, Micro-/macroporous ceramics from preceramic precursors, *J. Am. Ceram. Soc.* 84 (10) (2001) 2252–2255.
- [22] T. Prenzel, M. Wilhelm, Kurosch Rezwan, Pyrolyzed polysiloxane membranes with tailorable hydrophobicity, porosity and high specific surface area, *Microporous Mesoporous Mater.* 169 (2013) 160–167.
- [23] R.W. O'Brien, B.R. Midmore, A. Lamb, R.J. Hunter, Electroacoustic studies of moderately concentrated colloidal suspensions, *Faraday Discuss. Chem. Soc.* 90 (1990) 301–312.
- [24] D. Hanaor, M. Michelazzi, C. Leonelli, C.C. Sorrell, The effects of carboxylic acids on the aqueous dispersion and electrophoretic deposition of ZrO₂, *J. Eur. Ceram. Soc.* 32 (2012) 235–244.
- [25] J.W. Moon, H.J. Hwang, M. Awano, K. Maeda, Preparation of NiO–YSZ tubular support with radially aligned pore channels, *Mater. Lett.* 57 (2003) 1428–1434.
- [26] M. Pulkin, D. Koch, G. Grathwohl, K. Rezwan, Hydroxyapatite/SiO₂ composites via freeze casting for bone tissue engineering, *S., Blindow, Advanced Engineering Materials*, 11, 2009, 875–884.
- [27] J.H. Eom, Y.W. Kim, S. Raju, Processing and properties of macroporous silicon carbide ceramics: a review, *J. Asian Ceram. Soc.* 1 (2013) 220–242.
- [28] T. Nishi, T.T. Wang, T.K. Kwei, Thermally induced phase separation behavior of compatible polymer mixture, *Macromolecules* 8 (2) (1975) 227–234.
- [29] B. Wicklein, A. Kocjan, G. Salazar-Alvarez, F. Carosio, G. Camino, M. Antonietti, L. Bergström, Thermally insulating and fire-retardant lightweight anisotropic foams based on nanocellulose and grapheme oxide, *Nat. Nanotechnol.* 10 (2015) 277–283.
- [30] U.G.K. Wegst, M. Schecter, A.E. Donius, P.M. Hunger, Biomaterials by freeze casting, *Phil. Trans. R. Soc. A* 368 (2010) 2099–2121.
- [31] J.H. Eom, Y.W. Kim, S. Raju, Processing and properties of macroporous silicon carbide ceramics: a review, *J. Asian Ceram. Soc.* 1 (2013) 220–242.
- [32] P. Greil, Polymer derived engineering ceramics, *Adv. Eng. Mater.* 2 (2000) 339–348.
- [33] R. Dominko, D.E. Conte, D. Hanzel, M. Gaberscek, J. Jamnik, Impact of synthesis conditions on the structure and performance of Li₂FeSiO₄, *J. Power Sour.* 178 (2008) 842–847.
- [34] M. Adam, M. Wilhelm, G. Grathwohl, Polysiloxane derived hybrid ceramics with nanodispersed Pt, *Microporous Mesoporous Mater.* 151 (2012) 195–200.